Biochem. J. (1983) **211**, 631–640
Printed in Great Britain

Analysis of progress curves

Interaction of pyruvate kinase from *Escherichia coli* with fructose 1,6-bisphosphate and calcium ions

Arnold BOITEUX,* Mario MARKUS, Theo PLESSER and Benno HESS
Max-Planck-Institut für Ernährungsphysiologie, 4600 Dortmund 1, Rheinlanddamm 201, Federal Republic of Germany

and Massimo MALCOVATI
Istituto di Chimica Biologica, Università di Pavia, Via T. Taramelli 1, 27100 Pavia, Italy

(*Received 27 January 1983/Accepted 10 February 1983*)

The influence of fructose 1,6-bisphosphate and Ca^{2+} on the kinetics of pyruvate kinase from *Escherichia coli* K12 was studied (at pH 7.0 and 25°C) by using the pH-stat method for the measurement of the reaction progress as well as initial-rate analysis. The data were analysed on the basis of a concerted model with three conformational states [Markus, Plesser, Boiteux, Hess & Malcovati (1980) *Biochem. J.* **189**, 421–433] by using a novel procedure for a computer-directed treatment of progress curves [Markus & Plesser (1976) *Biochem. Soc. Trans.* **4**, 361–364]. By addition of fructose 1,6-bisphosphate the sigmoid kinetics with respect to phosphoenolpyruvate and Mg^{2+} is abolished and the activity of the enzyme is described by classical saturation kinetics. This is explained by exclusive binding of fructose 1,6-bisphosphate at an allosteric site of the conformational state that forms the active complex. We observe that Ca^{2+} is an activator of the enzyme at low Mg^{2+} and Ca^{2+} concentrations; otherwise it is an inhibitor. These effects can be understood by assuming that Ca^{2+} has the same binding properties as Mg^{2+}, although it does not allow a catalytic turnover.

In the presence of Mg^{2+}, or Mn^{2+} and K^+, pyruvate kinase (EC 2.7.1.40) catalyses the transphosphorylation from phosphoenolpyruvate to ADP, producing ATP and pyruvate. In a previous paper (Markus *et al.*, 1980) we described the kinetics of pyruvate kinase (Type I) from *Escherichia coli* K12 J53 in the regulatory region of the four-dimensional concentration space of phosphoenolpyruvate, ADP, Mg^{2+} and ATP with a quasi-equilibrium model implying three conformational states and four protomers, which is an extension of the concerted model of Monod *et al.* (1965). Only one conformational state forms the catalytically active complex with phosphoenolpyruvate, ADP and Mg^{2+}. A second conformational state binds ADP and Mg^{2+}. Binding of Mg^{2+} to this state causes strong inhibition at high Mg^{2+} concentrations, because this state is not catalytically active. In the absence of ligands, most of the enzyme is in a third state that can bind ADP at the active site and ATP as well as MgATP at an allosteric site. It is known that fructose 1,6-bisphosphate transforms in the enzyme of *E. coli* the sigmoid dependence of the enzymic reaction rate on phosphoenolpyruvate and magnesium into a Michaelis–Menten response (Malcovati & Kornberg, 1969; Waygood & Sanwal, 1974). In order to determine the mode of interaction of fructose 1,6-bisphosphate in the model, we analysed its influence on the overall kinetics of the enzyme and included calcium ions in our study as an additional ligand of possible regulatory significance.

Note below that when we write 'Mg_{total}' or 'total magnesium' we refer to the sum of chelated and unchelated magnesium atoms. We write 'Mg^{2+}' when we refer to the unchelated magnesium ions. For calcium we use an analogous nomenclature.

* To whom correspondence and reprint requests should be addressed.

Material and methods

Recording and analysis of progress curves

Details concerning materials and methods are the same as those given previously (Markus *et al.*, 1980), if not stated otherwise. Techniques and applications of progress-curve measurements have been described by Boiteux *et al.* (1981).

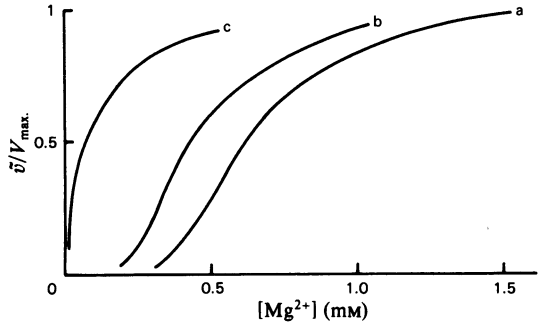

Fig. 1. *Reaction rates (normalized with respect to the maximal rate) as a function of Mg^{2+} concentration*
The curves were drawn from the computer output after numerical differentiation of measured progress curves. The conditions were: $[Pyr\text{-}P_{total}] = 30$ mM, $[ADP_{total}] = 30$ mM, $[Mg_{total}] = 12$ mM. Curve a, $[FBP_{total}] = 0$ mM; curve b, $[FBP_{total}] = 0.1$ mM; curve c, $[FBP_{total}] = 5$ mM. Abbreviations used: FBP, fructose 1,6-bisphosphate; Pyr-P, phosphoenolpyruvate).

The progress of the reaction was monitored by titration of the H^+ absorbed in the phosphate-transfer process. The measured signal was the volume of the titrant solution (100 mM-HCl and 100 mM-KCl) as a function of time. The main source of errors the propagation of errors in the initial concentrations of the substrates involved. We showed by replicate measurements (Markus *et al.*, 1980) that the resulting systematic errors are approximately proportional to the measured signal and that the S.D. of these errors divided by the measured signal is 0.053.

The course of the reaction was first inspected qualitatively by computation of the instantaneous reaction rates obtained from the derivatives of a spline function approximation. The approximation was performed by the subroutine TSO1A of the Harwell Subroutine Library (1973). An example of this evaluation procedure is given in Fig. 1, where each instantaneous reaction rate $\bar{v}$ corresponds to a different instantaneous concentration of Mg^{2+} because, with the total magnesium concentration being constant during the progress of the reaction, the product ATP chelates more Mg^{2+} than the substrates and the concentration of Mg^{2+} varies during the reaction accordingly. The initial conditions for the experiments in Fig. 1 are such that the consumption of the substrates and the accumulation of ATP within the measuring time have minor effects as compared with the effect of the variation of Mg^{2+}. The Figure thus shows the kinetics quite well.

A quantitative analysis was then performed by fitting the measured volume of the titrant solution by the volume obtained from the numerically integrated rate law under consideration of all variations of ligands. In these calculations we considered the buffer capacity of the solution by computing, at any given time point, the amount of H^+ bound to the solutes. Also, we accounted for the dilution of the enzyme and ligands due to the addition of the titrant solution.

In order to compute the concentrations of Mg^{2+}, of Mg^{2+}-free ligands and of the magnesium chelates, we used the same dissociation constants for the cation product and the cation–substrate complexes as in our previous work (Markus *et al.*, 1980). Additionally, we used the following constants given by McGilvery (1965) (FBP = fructose 1,6-bisphosphate):

$$\frac{[FBP^{4-}][Mg^{2+}]}{[MgFBP^{2-}]} = 2.0\,\text{mM} \quad (1)$$

$$\frac{[FBP^{4-}][H^+]}{[HFBP^{3-}]} = 1.74 \times 10^{-4}\,\text{mM} \quad (2)$$

$$\frac{[HFBP^{3-}][H^+]}{[H_2FBP^{2-}]} = 1.1 \times 10^{-3}\,\text{mM} \quad (3)$$

$$\frac{[HFBP^{3-}][Mg^{2+}]}{[MgHFBP^{-}]} = 7.59\,\text{mM} \quad (4)$$

When optimizing, we weighted the residuals with the reciprocal of the measured volume, taking into account that the error was approximately proportional to this volume, as was shown by the replicates discussed above.

Analysis of the influence of fructose 1,6-bisphosphate

Progress-curve experiments were performed in a reaction mixture containing, at zero time, in a known volume (approx. 1 ml) of 100 mM-KCl solution, the ligand concentrations given in Table 1. The initial concentrations were selected on the basis of the known properties of the enzyme to cover the regulatory region of the concentration space. The initial concentration of ATP was equal to zero in all experiments. The rate-determining essential ligands are indicated in the last column of Table 1. The additions of fructose 1,6-bisphosphate in the different experiments were chosen in such a way that the sigmoidicity with respect to phosphoenolpyruvate or Mg^{2+} is partially abolished at the smaller fructose 1,6-bisphosphate additions and fully abolished at the highest fructose 1,6-bisphosphate additions. The reaction was started by the addition of 5 μl of pyruvate kinase solution, containing 9.44 μg of

Table 1. *Total initial concentrations of the ligands in progress-curve experiments*
Abbreviations used: Pyr-P, phosphoenolpyruvate; FBP, fructose 1,6-bisphosphate.

Expt. no.	[Pyr-P_{total}] (mM)	[ADP_{total}] (mM)	[Mg_{total}] (mM)	[FBP_{total}] (mM)	Rate-determining essential ligand(s)
1	10	20	18	0.03	Pyr-P
2	10	20	18	1	Pyr-P
3	50	20	40	1	ADP
4	30	30	12	0.1	Mg^{2+}
5	30	30	12	5	Mg^{2+}
6	14	12	30	0.03	Pyr-P, ADP
7	14	12	30	2	Pyr-P, ADP
8	12	25	10	0.03	Pyr-P, Mg^{2+}
9	12	25	10	0.1	Pyr-P, Mg^{2+}
10	12	25	10	2	Pyr-P, Mg^{2+}
11	25	12	11	0.1	ADP, Mg^{2+}
12	25	12	11	2	ADP, Mg^{2+}
13	15	12	10	0.03	Pyr-P, ADP, Mg^{2+}
14	15	12	10	0.1	Pyr-P, ADP, Mg^{2+}
15	15	12	10	2	Pyr-P, ADP, Mg^{2+}

enzyme. Measurements were performed at 25°C and pH 7.0.

After the progress curves for the conditions given in Table 1 were measured, maximization of the determinant of Fisher's information matrix (Markus & Plesser, 1976) led to an experimental design in the concentration region defined by the following constraints: $v > 0.05 V_{max.}$, $0 < [\text{phosphoenolpyruvate}_{total}] < 50$ mM, $0 < [ADP_{total}] < 30$ mM, $0 < [ATP_{total}] < 30$ mM, $0.1 < [Mg^{2+}] < 20$ mM, $0 < [\text{fructose 1,6-bisphosphate}_{total}] < 5$ mM. Further progress-curve measurements over this concentration range did not add any substantial information, in terms of Fisher's information matrix, about the dependence of the reaction rate on the ligands. Owing to the limitations in computer capacity, a choice of the data points to be evaluated on the progress curves had to be performed. This choice was also done by using Fisher's information matrix. The final set of data points corresponds to saturation of the information content (Markus & Plesser, 1976).

Analysis of the influence of Ca^{2+}

The influence of Ca^{2+} on the enzyme was analysed photometrically with initial-rate measurements at 25°C. The assay mixture contained, in a final volume of 1 ml: 50 mM-triethanolamine/HCl buffer, pH 7.00, and 0.3 mM-NADH. The concentrations of phosphoenolpyruvate, ADP, KCl, mercaptoethanol, calcium and magnesium are given in the legends to, and on the abscissae of, Figs. 3, 4, 5 and 6. The reaction was started by the addition of 0.04 μg of pyruvate kinase. The activity of lactate dehydrogenase was taken to be $\geqslant$50 times higher than the pyruvate kinase activity to guarantee proportionality between enzyme concentration and reaction velocity.

Results and model interpretation

Fructose 1,6-bisphosphate

The influence of magnesium on the interaction of fructose 1,6-bisphosphate with pyruvate kinase, previously investigated for the enzyme from yeast by Haeckel *et al.* (1968), can be shown by plotting the Mg^{2+}-dependence of the rates obtained from progress curves nos. 4 and 5 from Table 1 and the corresponding curve in the absence of fructose 1,6-bisphosphate. The instantaneous reaction rates ($\tilde{v}$) used in Fig. 1 were calculated from the slopes of the tangents of the progress curves (see the Materials and methods section). Fig. 1 shows clearly that the rate is a sigmoid function of Mg^{2+} in the absence of fructose 1,6-bisphosphate (curve a). The rate displays a hyperbolic curve if the activator fructose 1,6-bisphosphate is present in saturating concentration (curve c). Increasing fructose 1,6-bisphosphate levels shift the Mg^{2+} concentration for the half-maximal rate to lower values. Lower concentrations of Mg^{2+} than those shown in Fig. 1 were not reached within the time of duration of the progress curve.

The abolition of the sigmoidicity by fructose 1,6-bisphosphate suggests that the latter ligand binds, at an allosteric site, more strongly to the catalytically active state R_1 than to other conformational states. The addition of fructose 1,6-bisphosphate thus displaces the various conformations towards the state R_1.

This observation could readily be incorporated into our previous results obtained in the absence of

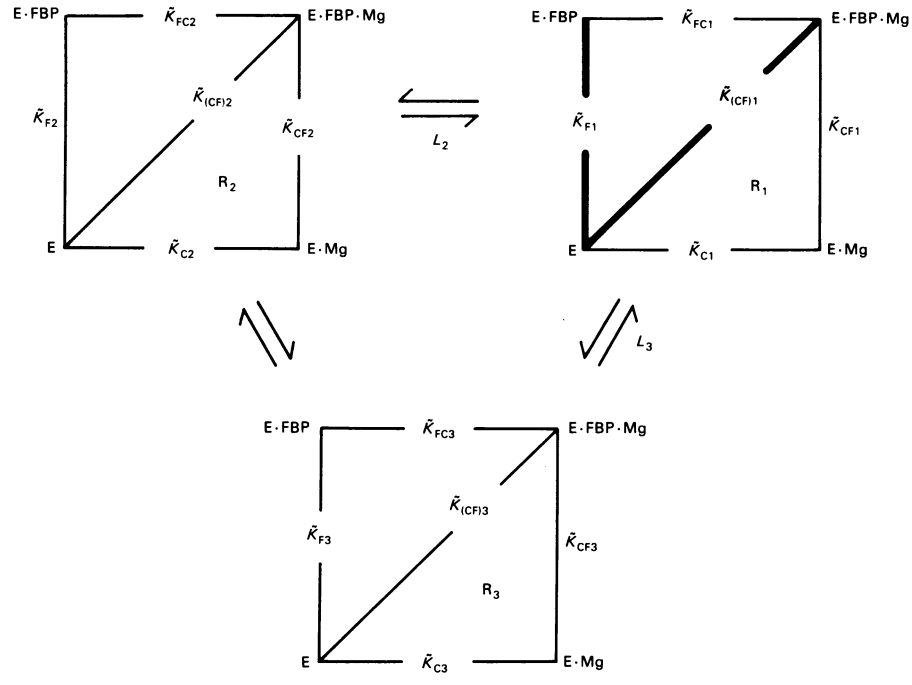

Scheme 1. *Binding scheme for the allosteric fructose 1,6-bisphosphate binding site*

The thin lines represent the general binding scheme considered before optimization. The thicker lines show the binding processes left over after optimization. The enzyme–ligand complexes and the dissociation constants, $\tilde{K}$, are shown at the vertices and edges respectively. The indices C and F refer to Mg^{2+} and uncomplexed fructose 1,6-bisphosphate, written in the order of binding to the enzyme. The last index (1, 2 and 3) refers to the conformational state. Abbreviation used: FBP, fructose 1,6-bisphosphate.

fructose 1,6-bisphosphate. An extension of the previous model (Markus *et al.*, 1980), allowing random binding of Mg^{2+}-free fructose 1,6-bisphosphate and Mg^{2+} at an allosteric site and assuming different dissociation constants for the different conformational states, yielded Scheme 1. Each vertex of the Scheme represents an enzyme–ligand complex. The dissociation constants describe the equilibria between the corresponding vertices. The indices C and F refer to Mg^{2+} and Mg^{2+}-free fructose 1,6-bisphosphate respectively, and are written in the order of binding of the ligands to the enzyme. The last index distinguishes between the conformational states. We assume that all enzyme species are in quasi-equilibrium. For the dissociation constants we use the symbols K, $\tilde{K}$ and $\tilde{\tilde{K}}$ when refering to binding at the active site, the allosteric ATP-binding site and the allosteric fructose 1,6-bisphosphate-binding site respectively.

This extension of the model is described by the dissociation constants $\tilde{\tilde{K}}_{C\nu}$, $\tilde{\tilde{K}}_{(CF)\nu}$ and $\tilde{\tilde{K}}_{F\nu}$ ($\nu = 1, 2, 3$). The rate law formulated in our previous work (Markus *et al.*, 1980) is modified by replacing L_ν ($\nu = 2, 3$) by the expression:

$$L_\nu \left(\frac{D_\nu}{D_1}\right)^4$$

where:

$$D_\nu = 1 + \frac{[Mg^{2+}]}{\tilde{\tilde{K}}_{C\nu}} + \frac{[MgFBP^{2-}] + [MgHFBP^{-}]}{\tilde{\tilde{K}}_{(CF)\nu}} + \frac{[FBP^{4-}] + [HFBP^{3-}]}{\tilde{\tilde{K}}_{F\nu}} \quad (5)$$

The total numbers of parameters to be determined is 17: eight parameters derived from our previous model, plus the nine independent parameters introduced above to describe the binding of fructose 1,6-bisphosphate.

In order to test this interpretation, the 15 progress curves defined by the initial conditions given in Table 1 were fitted simultaneously with the 14 curves and the discrimination experiments measured in the

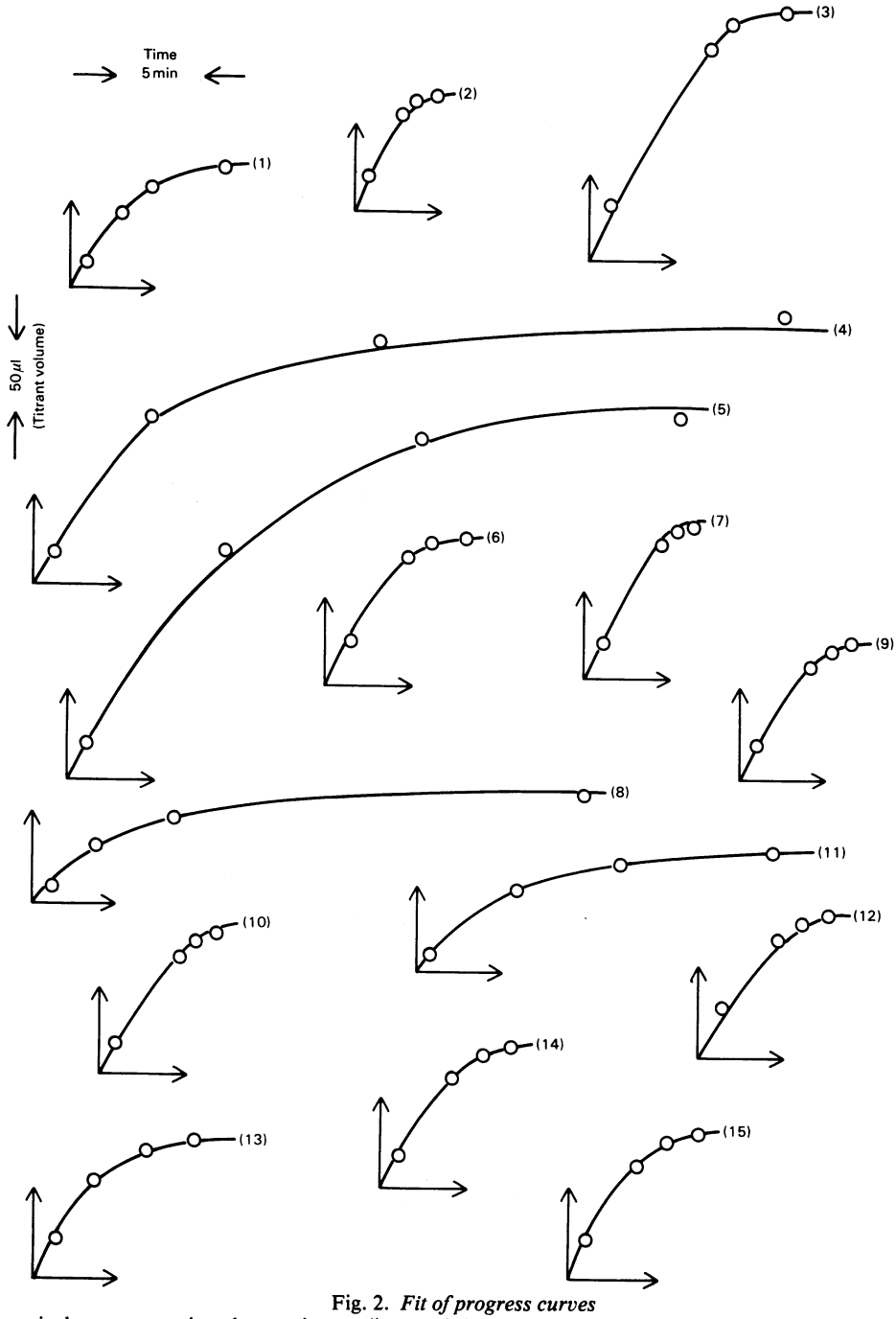

Fig. 2. *Fit of progress curves*

The theoretical curves are given by continuous lines and the evaluated experimental points by open circles (O). The initial concentrations are given in Table 1.

absence of fructose 1,6-bisphosphate, which are given in Fig. 8 of our previous paper (Markus *et al.*, 1980). At the minimum of the weighted sum of squares we obtained an S.D. of the weighted residuals equal to 0.056. This value is comparable with the experimental error (see the Materials and methods section). Fig. 2 compares the experiments obtained for the initial conditions defined in Table 1 and the results of the fit procedure with the model. The fit with the experiments in the absence of fructose

Table 2. *Optimized parameters*
The nomenclature is taken from our previous paper (Markus *et al.*, 1980).

No.	Parameter	Values: [FBP] ≠ 0 (present work)	Values: [FBP] = 0 (Markus *et al.*, 1980)	Dimension	Explanation
1	k_1	$(4.8 \pm 0.2) \times 10^4$	$(5.1 \pm 0.2) \times 10^4$	min^{-1}	Catalytic-centre activity ('turnover number') of the conformational state R_1.
2	z	0.309 ± 0.003	0.315 ± 0.006	—	Proportionality constant between percentage increase in activity and percentage decrease in ionic strength.
3	$\tilde{K}_{Q3}$	22.5 ± 1.4	22.4 ± 2.1	mM	Dissociation constant of ATP or MgATP at an allosteric site of the conformational state R_3.
4	$K_{C2}/\sqrt[4]{L_2}$	0.72 ± 0.14	0.59 ± 0.19	mM	K_{C2}, dissociation constant of Mg^{2+} at the conformational state R_2; L_2, equilibrium constant between the conformational states R_2 and R_1 in a ligand-free solution.
5	K_{B1}	0.26 ± 0.06	0.18 ± 0.05	mM	Dissociation constant of ADP at conformational state R_1.
6	K_{A1}	0.31 ± 0.09	0.31 ± 0.18	mM	Dissociation constant of Pyr-P at conformational state R_1.
7	$K_{A(CB)1}$	0.69 ± 0.15	0.44 ± 0.25	mM	Dissociation constant of MgADP after binding of Pyr-P at conformational state R_1.
8	L_3	$(1.0 \pm 0.4) \times 10^3$	$(1.15 \pm 0.7) \times 10^3$	—	Equilibrium constant between conformational states R_3 and R_1 in a ligand-free solution.
9	$\tilde{K}_{F1}$	0.19 ± 0.03		mM	$(= \tilde{K}_{(CF)1})$, dissociation constant of FBP or MgFBP at an allosteric site of the conformational state R_1.

Correlation matrix ([FBP] ≠ 0, present work):

2	−0.22	1						
3	0.23	−0.79	1					
4	−0.09	−0.48	0.61	1				
5	0.18	−0.04	−0.08	0.41	1			
6	−0.11	0.15	−0.18	0.54	0.80	1		
7	0.41	−0.74	0.78	0.17	−0.15	−0.56	1	
8	−0.02	0.59	−0.80	−0.81	0.02	−0.20	−0.33	1
9	−0.04	−0.13	0.10	0.00	−0.17	−0.15	0.10	−0.15
	1	2	3	4	5	6	7	8

These are the correlation coefficients of the logarithms of the parameters.

1,6-bisphosphate (see Fig. 8 of Markus *et al.*, 1980) was not appreciably different if performed independently or simultaneously with the experiments shown in Fig. 2.

After optimization, we found that $\tilde{K}_{C\nu}$, $\tilde{K}_{(CF)\nu}$ and $\tilde{K}_{F\nu}$ can be set to infinite for $\nu = 2, 3$, i.e. fructose 1,6-bisphosphate only binds to the state R_1. Furthermore, $\tilde{K}_{C_1}$ can also be set to infinity and $\tilde{K}_{(CF)1} = \tilde{K}_{F1}$, i.e. the dissociation constant of fructose 1,6-bisphosphate with the enzyme is the same whether fructose 1,6-bisphosphate is chelated with Mg^{2+} or not. The activation by fructose 1,6-bisphosphate thus depends only on the concentration of total fructose 1,6-bisphosphate, the dissociation constant with the state R_1 being $\tilde{K}_{F1}$.

The final set of optimized parameters with the errors and correlations obtained from the co-variance matrix is summarized in Table 2. These parameter values may to some extent depend on the chosen set of dissociation constants for the cation–ligand complexes, as already mentioned in our previous paper (Markus *et al.*, 1980). For comparison, the parameters obtained previously (Markus *et al.*, 1980) in the absence of fructose 1,6-bisphosphate are given as well. In this extended investigation, the parameters are almost unchanged; their errors, however, become definitively smaller. The correlation coefficients shown in the bottom of Table 2 may assume values between −1 and +1, indicating the degree of dependency of the parameter values on each other. These coefficients indicate, in general, lower correlations than in our previous work.

Calcium ions

We carried on the investigation with Mg^{2+} by analysing the influence of Ca^{2+} on the kinetics as a possible bivalent competitor. Initial-rate analysis shows that 10 mM-Ca_{total} completely abolishes the sigmoid dependency of the reaction rate on Mg_{total} in the absence of fructose 1,6-bisphosphate and yields

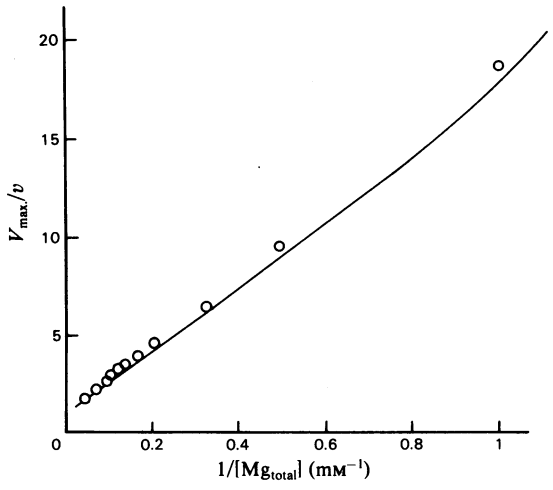

Fig. 3. *Lineweaver–Burk plot for total magnesium in the presence of Ca^{2+}*

The continuous line and the open circles (O) show the model prediction and the initial-rate measurements respectively. The conditions were: [Pyr-P_{total}] = 8 mM, [ADP_{total}] = 20 mM, [Ca_{total}] = 10 mM, [KCl] = 100 mM, [mercaptoethanol] = 5 mM. Abbreviation used: Pyr-P, phosphoenolpyruvate.

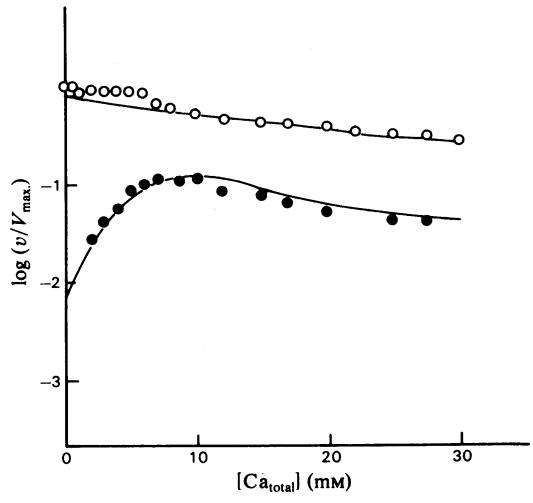

Fig. 4. *Effect of calcium on the reaction rate*

The continuous lines and the circles (●, O) show the model prediction and the initial-rate measurements respectively. The conditions were: [Pyr-P_{total}] = 8 mM, [ADP_{total}] = 20 mM, [Mg_{total}] = 2 mM (●) or 20 mM (O), [mercaptoethanol] = 5 mM, [KCl] = 100 mM. Abbreviation used: Pyr-P, phosphoenolpyruvate.

hyperbolic saturation kinetics, as shown in Fig. 3. The maximal activity remains unchanged.

A more detailed picture of the interaction of Ca^{2+} and Mg^{2+} ions with the enzyme is obtained in the experimental results described in Fig. 4. Whereas any concentration of calcium inhibits the enzyme in the presence of high magnesium (total 20 mM) (upper trace), an activation is observed at lower magnesium and lower calcium concentrations (lower trace). These data clearly show that the calcium and magnesium action is not simply competitive, but also, at lower concentrations, co-operative. We tested the model given above, adding the following features.

(1) Mg^{2+} and Ca^{2+} occupy the same binding sites [magnetic-resonance studies (Mildvan & Cohn, 1965) indicate interchangeable occupancy for Mg^{2+} and Ca^{2+}].

(2) Dissociation constants for Ca^{2+} complexes with the enzyme and with the ligands are identical with those of their Mg^{2+} counterparts (simplest assumption; needs verification by further experiments).

(3) Replacement of Mg^{2+} by Ca^{2+} in the active-site complex leads to an inactive complex (simplest model for Ca^{2+} inhibition).

A straightforward simulation with these additional features yielded the drawn lines given in Figs. 3 and 4, demonstrating a close agreement between simulation and experimental results (for a detailed discussion, see below).

For further testing of our model assumptions, we measured the reaction-rate-dependence on the concentration of Ca^{2+} with [FBP_{total}] = 5 mM and at constant concentrations of substrates free of bivalent cations. These measurements are shown in Fig. 5. In order to increase the accuracy of this model test, we kept the ion strength constant at 300 mM by additions of KCl. According to our model, at such a high fructose 1,6-bisphosphate concentration, the enzyme should exist only in the state R_1. The reaction rate thus obeys the equation (Markus *et al.*, 1980):

$$v = \frac{V_{max.}\dfrac{[\text{Pyr-P}][\text{MgADP}]}{K_{A1}K_{A(CB)1}}}{1+\dfrac{[\text{ADP}]}{K_{B1}}+\dfrac{[\text{Pyr-P}]}{K_{A1}}+\dfrac{[\text{Pyr-P}][\text{MgADP}]}{K_{A1}K_{A(CB)1}}+\dfrac{[\text{Pyr-P}][\text{CaADP}]}{K_{A1}K_{A(CB)1}}} \quad (6)$$

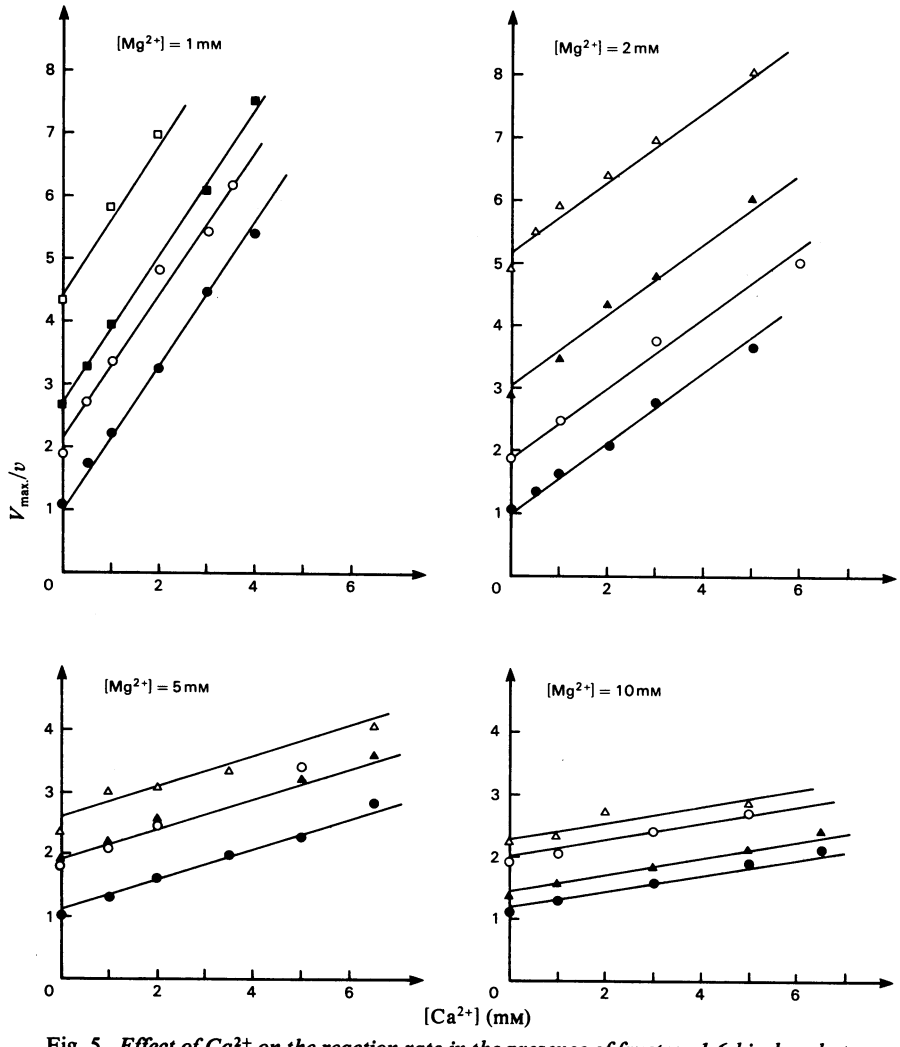

Fig. 5. *Effect of Ca^{2+} on the reaction rate in the presence of fructose 1,6-bisphosphate*
The general conditions were: $[FBP_{total}] = 5$ mM, [mercaptoethanol] = 1 mM. KCl was added to hold the ionic strength constant at 300 mM. The concentration of free calcium was varied while the concentrations of unchelated Pyr-P and ADP were held constant (□, ADP=0.4 mM, [Pyr-P]=0.2 mM; ■, [ADP]=0.4 mM, [Pyr-P]=10 mM; △, [ADP]=0.2 mM, [Pyr-P]=0.2 mM; ▲, [ADP]=0.2 mM, [Pyr-P]=10 mM; ○, [ADP]=3 mM, [Pyr-P]=0.2 mM; ●, [ADP]=3 mM, [Pyr-P]=10 mM). Abbreviations used: Pyr-P, phosphoenolpyruvate; FBP, fructose 1,6-bisphosphate.

Pyr-P and ADP are the substrates free of bivalent cations. K_{A1} and K_{B1} are the dissociation constants of the complexes formed by the free enzyme with Pyr-P and ADP respectively. $K_{A(CB)1}$ is the dissociation constant for the complex formed by E·Pyr-P and MgADP, which is equal to that involving CaADP, according to feature (2) above. Owing also to this feature, we can write:

$$[CaADP]/[MgADP] = [Ca^{2+}]/[Mg^{2+}]$$

Taking the reciprocal value on both sides of eqn. (6) yields:

$$\frac{V_{max.}}{v} = f([Pyr\text{-}P], [Mg^{2+}], [ADP]) + \frac{[Ca^{2+}]}{[Mg^{2+}]} \quad (7)$$

where the function f does not depend on $[Ca^{2+}]$. Eqn. (7) shows that a plot of $V_{max.}/v$ versus $[Ca^{2+}]$ leads to a straight line, its slope being $1/[Mg^{2+}]$, which is independent of [Pyr-P] and [ADP]. Our

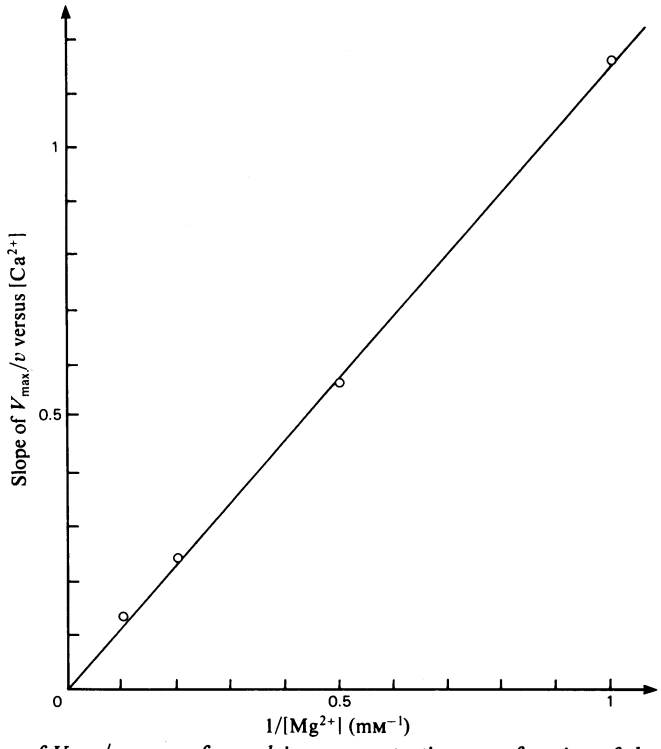

Fig. 6. *Replot of the slope of $V_{max.}/v$ versus free calcium concentration as a function of the reciprocal free-magnesium concentration*

The four points (O) correspond to the slope of the four sets of curves (one set for each concentration of Mg^{2+}) shown in Fig. 5.

measurements show that this is indeed the case (see Fig. 5). This result confirms our assumption that no turnover is possible when Ca^{2+} instead of Mg^{2+} binds at the active site, because we would have obtained no straight lines otherwise, as can be seen by inspection of the rate law. If the slopes of the straight lines shown in Fig. 5 are replotted as a function of $1/[Mg^{2+}]$, one should obtain again a straight line with a slope equal to 1. Fig. 6 shows that the experiments confirm this linear dependence, the slope being 1.15, which is very close to the predicted value of 1. One should bear in mind, however, that this test of the model is restricted to the state R_1 of the enzyme, as no such linearizations are possible when other enzymic states are present.

Discussion

Fructose 1,6-bisphosphate

There is good agreement between the parameter values shown in Table 2 and the values obtained from the literature, as well as our own values (summarized in Markus *et al.*, 1980). There are, however, discrepancies in a comparison with those data obtained from binding studies with fructose 1,6-bisphosphate by Waygood *et al.* (1976). Those authors obtained $\tilde{K}_{F1} = 0.026 \pm 0.002$ mM, $\tilde{K}_{F3} = 0.5 \pm 0.1$ mM, $L_3 = 68 \pm 25$. This disagreement with our results could be explained by the fact that the binding studies were performed at $[KCl] = 0$. The KCl concentration substantially affects the action of fructose 1,6-bisphosphate on the enzyme (Hess & Haeckel, 1967).

We found previously that magnesium can function as an activator as well as an inhibitor (Markus *et al.*, 1980). The inhibition by magnesium can occur by two different mechanisms depending on the distribution of the ligands: (1) decreasing the concentration of unchelated ADP and phosphoenolpyruvate by complex-formation, and (2) shifting of the equilibrium towards the enzymically inactive state, R_2 (high Mg^{2+} concentrations). Comparing our results with observations on pig liver pyruvate kinase reveals striking similarities. Kutzbach *et al.* (1973) measured the inhibitory effect of magnesium on this enzyme with and without fructose 1,6-bisphosphate additions. In the presence of fructose 1,6-bisphosphate, where the enzyme exists only in one conformational state, they observed a decrease in enzyme activity to one-third by addition of 50 mM-Mg_{total}. Obviously, this is due to the formation of Mg^{2+}–substrate complexes. In the absence of fructose 1,6-bisphosphate, more than one con-

formational state may be present. Owing to this fact, these authors observed in their study that the same concentration of Mg_{total} produces a much greater decrease in enzymic activity, namely to one-tenth. This suggests that, besides the inhibition of the enzyme by formation of Mg^{2+}-substrate complexes, an inhibitory effect involving binding of Mg^{2+} to an inactive conformational state may also take place in pyruvate kinase from liver.

Identical properties of enzymes genetically as different as pyruvate kinase from bacteria and mammals strongly suggest that the two mechanisms outlined above for the inhibition by magnesium are of general significance.

Calcium ions

Although no fitting was performed for parameter redetermination and although the assumption of identical dissociation constants for calcium and magnesium complexes is only approximately correct, there is good agreement between the simulation and the experimental results obtained for the interaction of calcium with the enzyme. The activation by calcium shown in the lower left of Fig. 4 is explained by the fact that, at the given distribution of ligands, Ca^{2+} in common with Mg^{2+} shifts the equilibrium towards the active state, R_1. Indeed, Fig. 3 shows an almost Michaelian response of the enzyme to Mg_{total}, indicating that, at the Ca_{total} concentration of 10mM, the equilibrium distribution of states is almost completely shifted towards the state R_1. Inhibition by calcium is mechanistically analogous to the inhibition by magnesium. Furthermore, Ca^{2+} inhibits the enzyme by competition with Mg^{2+} at the active site. Kachmar & Boyer (1953) and Genin & Andreev (1975) observed the inhibition, but not the activation, by calcium in the case of other pyruvate kinases. This is explained by the fact that those authors investigated enzymes obeying Michaelis–Menten kinetics, so that no conformational changes due to the addition of Ca^{2+} could be recorded. Haeckel *et al.* (1968) observed activation by calcium under limiting magnesium concentrations in the case of yeast pyruvate kinase. This indeed should be expected from our model. Also, in accordance with our model considerations is the observation that the sigmoid dependence on Mg_{total} of the reaction rate of yeast pyruvate kinase becomes hyperbolic on addition of $[Ca_{total}]$ in the order of 6mM (H.-J. Wieker, personal communication).

Conclusion

Our quantitative analysis of the interaction of fructose 1,6-bisphosphate with the enzyme yields an excellent consistency with the kinetic model of pyruvate kinase of *E. coli* described previously (Markus *et al.*, 1980) and corroborates the mechanism of exclusive allosteric binding of total fructose 1,6-phosphate to the enzyme observed in the case of yeast (Johannes & Hess, 1973). In addition, our study offers two separate mechanisms accounting for the interaction of calcium with the enzymic reaction. First, there is the interaction with the substrates involved and second, the interaction with the enzymic conformations. The latter interaction might displace Mg^{2+} on the active site of the state R_1, shift the conformational equilibrium towards the abortive state R_2, or shift the equilibrium to the state R_1 that forms the active complex. This last-mentioned effect explains the observation that though calcium is an inhibitor it also can activate the enzyme at low magnesium and calcium concentrations; under these conditions the Ca^{2+}-induced shift of the equilibrium to the active conformation outweighs its inhibitory effect.

It is noteworthy that the classical initial-rate analysis of kinetic mechanisms can readily be detailed by reaction progress analysis as shown here, yielding considerable additional insight into the overall mechanism of the enzyme.

We thank Dr. H.-J. Wieker for fruitful discussions and Mr. H. Schlüter, Mr. E. Hickl and Mr. K. Dreher for technical assistance.

References

Boiteux, A., Markus, M., Plesser, Th. & Hess, B. (1981) in *Kinetic Data Analysis: Design and Analysis of Enzyme and Pharmacokinetic Data* (Endrenyi, L., ed.), pp. 341–353, Plenum Press, New York

Genin, M. S. & Andreev, V. S. (1975) *Biokhimiya* **40**, 885–889

Haeckel, R., Hess, B., Lauterborn, W. & Wuester, K. H. (1968) *Hoppe-Seyler's Z. Physiol. Chem.* **349**, 699–714

Hess, B. & Haeckel, R. (1967) *Nature (London)* **214**, 848–849

Johannes, K.-J. & Hess, B. (1973) *J. Mol. Biol.* **76**, 181–207

Kachmar, J. F. & Boyer, P. D. (1953) *J. Biol. Chem.* **200**, 669–682

Kutzbach, K. J., Bischofsberger, H., Hess, B. & Zimmermann-Telschow, H. (1973) *Hoppe-Seyler's Z. Physiol. Chem.* **354**, 1473–1489

Malcovati, M. & Kornberg, H. L. (1969) *Biochim. Biophys. Acta* **178**, 420–423

Markus, M. & Plesser, Th. (1976) *Biochem. Soc. Trans.* **4**, 361–364

Markus, M., Plesser, Th., Boiteux, A., Hess, B. & Malcovati, M. (1980) *Biochem. J.* **189**, 421–433

McGilvery, R. W. (1965) *Biochemistry* **4**, 1924–1930

Mildvan, A. S. & Cohn, M. (1965) *J. Biol. Chem.* **240**, 238–246

Monod, J., Wyman, J. & Changeux, J.-P. (1965) *J. Mol. Biol.* **12**, 88–118

Waygood, E. B. & Sanwal, B. D. (1974) *J. Biol. Chem.* **249**, 265–274

Waygood, E. B., Mort, J. S. & Sanwal, B. D. (1976) *Biochemistry* **15**, 277–282